Interference Steering to Manage Interference in IoT

Zhao Li, *Member, IEEE*, Yinghou Liu, Kang G. Shin, *Life Fellow, IEEE*, Jia Liu, *Member, IEEE*, and Zheng Yan, *Senior Member, IEEE*

***Abstract*—Internet of Things (IoT) is a new paradigm that involves the interconnection of thousands of devices and home appliances. Due to the scarcity of the spectrum suitable for wireless electromagnetic transmission, many communication systems and devices are close to each other, or even overlapping in spectrum, thus incurring complicated interference situations. Therefore, interference in IoT is worthy of thorough investigation and should be well addressed. There have been numerous interference management (IM) proposals at the interfering transmitter or the interfered transmitter/receiver separately or cooperatively. Moreover, the existing IM schemes rely mainly on the use of channel state information (CSI). However, in some communication scenarios, the option to adjust the interferer is not available, and, in the case of downlink transmission, it is always difficult or even impossible for the interfered receiver to acquire necessary information for IM. Based on the above observations, we first propose a novel IM technique, called *interference steering* (IS). By making use of both CSI with respect to and data carried in the interfering signal, IS generates a signal to modify the spatial feature of the original interference, so that the steered interference at the interfered receiver is orthogonal to its intended signal. We then apply IS to a wireless local area network (WLAN)-based IoT in which the same frequency band is reused by adjacent basic service sets (BSSs) with overlapping areas. With IS, multiple nearby access points (APs) could simultaneously transmit data on the same channel to their mobile stations (STAs), thus enhancing spectrum reuse. Our in-depth simulation results show that IS significantly improves network SE over existing IM schemes.**

***Index Terms*—Antenna arrays, costs, interference, Internet of Things (IoT), signal processing.**

I. Introduction

NEXT-GENERATION (also known as IMT-2020 or 5G) mobile wireless networks are characterized by high data rate, high system capacity, and massive device connectivity [1]. Wireless networks circa 2020 are expected to be 1000× larger in capacity and capable of connecting 100 billion devices [2]. Internet of Things (IoT), which has recently drawn more attention due to its ability to achieve the interconnection of massive physical devices, is a competitive 5G technology for massive machine-type communication scenarios [3]. However, due to the scarcity of the spectrum suitable for wireless electromagnetic transmission, many various existing and emerging communication systems, as well as mobile devices, are close to each other, or even overlapping in spectrum, which inevitably results in intensive interference [3], [4]. Moreover, in order to enable densely populated basic service sets (BSSs) or access points (APs) to serve an increasing number of users and provide diverse mobile services, efficient spectrum utilization policies and techniques should be developed. However, interference will rise with the increase of spectrum utilization, and must be well addressed so as to achieve high spectrum efficiency in IoT [3], [5]–[8].

Stankovic [5] provided a basis for discussing open research problems in IoT, and pointed out that research in IoT relies on underlying technologies, such as real-time computing, machine learning, security, signal processing, etc. It was highlighted in [5] that interference arises from many issues, and thus its management is crucial to IoT. By noting that in order to facilitate the harmonic and fair coexistence in wireless heterogeneous networks, it is important to eliminate narrowband IoT (NB-IoT) interference to long-term evolution (LTE) systems, Liu *et al.* [3] formulated a novel sparse machine learning-based probabilistic framework of NBI recovery. Wang and Fapojuwo [6] presented the design and performance evaluation of successive interference cancellation (SIC)-based pure Aloha (PA) for IoT networks. In each iteration of SIC, the receiver tries to receive as many packets as possible, and then the received packets can be used for interference cancellation (IC) in the next iteration of SIC. In [7], a resource orchestration scheme between edge gateways (EGs) and edge server (ES) and/or among EGs based on a Lagrangian and the Karush–Kuhn–Tucker condition was proposed. The scheme allocates optimal resources by considering the computing capacities of EGs and ES and manages interference among the EGs to maximize the efficiency of IoT systems. Liu *et al.* [8] was concerned with a machine learning approach to cancel the interference for cognitive IoT (C-IoT) in the concurrent spectrum access model, where the C-IoT

Manuscript received June 27, 2019; revised August 16, 2019; accepted August 23, 2019. Date of publication September 4, 2019; date of current version December 11, 2019. This work was supported in part by the China 111 Project under Grant B16037, in part by the NSFC under Grant 61672410 and Grant 61802292, in part by the Project of Cyber Security Establishment with Inter University Cooperation, in part by the Secom Science and Technology Foundation, and in part by the U.S. National Science Foundation under Grant CNS-1317411. *(Corresponding author: Zhao Li.)*

Z. Li is with the School of Cyber Engineering, Xidian University, Xi'an 710126, China, and also with the Shaanxi Key Laboratory of Information Communication Network and Security, Xi'an University of Posts and Telecommunications, Xi'an 710121, China (e-mail: zli@xidian.edu.cn).

Y. Liu is with the School of Telecommunications, Xidian University, Xi'an 710071, China.

K. G. Shin is with the Electrical Engineering and Computer Science Department, University of Michigan, Ann Arbor, MI 48109 USA.

J. Liu is with the Center for Cybersecurity Research and Development, National Institute of Informatics, Tokyo 101-8430, Japan.

Z. Yan is with the School of Cyber Engineering, Xidian University, Xi'an 710126, China (e-mail: zyan@xidian.edu.cn).

Digital Object Identifier 10.1109/JIOT.2019.2939255

2327-4662 © 2019 IEEE. Personal use is permitted, but republication/redistribution requires IEEE permission.
See http://www.ieee.org/publications_standards/publications/rights/index.html for more information.

system is noncooperative and has very limited knowledge on the interference. Therefore, interference is critical to the application of IoT and thus warrants a thorough investigation.

There have been numerous promising proposals to manage interference, which can be classified into two types. The first is isolating mutually interfering transmissions via resource partition, such as fractional frequency reuse (FFR), soft frequency reuse (SFR) [9], enhanced intercell interference coordination (eICIC) [10], etc. However, these mechanisms may cause degradation of spectrum efficiency. The second type is employing various signal processing techniques, such as zero-forcing beamforming (ZFBF) [11], zero-forcing (ZF) reception [12], coordinate multipoint (CoMP) [13], IC [14], interference alignment (IA)[1] [17], interference neutralization (IN) [18]–[22], etc., to support concurrent transmission of multiple interfering signals.

Of these signal processing methods, IA-based scheme mapped multiple interfering signals into a finite subspace by preprocessing interferences at the Tx, so that the desired signal(s) may be sent through a subspace without attenuation [15]–[17]. IA is highly dependent on system parameters, such as the number of transmitters and receivers and configuration of transmit/receive antennas [17]. That is, although IA emerges as a promising interference management (IM) scheme, its applicability is still limited by the requirement of DoFs. Moreover, given one DoF for IM at the interfered Rx side, IA is not applicable if multiple interferences are from an identical transmitter. This is because if the interfering signals originating from the same source are aligned in one direction, they will also overlap with each other at their intended receivers, thus becoming indistinguishable. IN has been under development in recent years [18]–[22]. It is a new IM mechanism found from, and inherent in interference networks with relays [19], [20]. IN strives to combine signals arriving via various paths in such a way that the interfering signals are canceled while preserving the desired signals [21]. It can be regarded as a distributed ZF of interference before the interfering signal reaches the undesired destination [22]. Chen *et al.* [21] constructed a linear distributed IN that encodes signals in both space and time for separate multiuser uplink-downlink two-way communications. In [22], an aligned IN was proposed in a multihop interference network formed by concatenation of two two-user interference channels. It provides a way to align interference terms over each hop in a manner that allows them to be canceled over the air at the last hop.

Note, however, that none of these existing IM methods are free of cost. For example, the channel state information (CSI) is required for implementing IA, ZF, and ZFBF, whereas both CSI with respect to and data carried in the interfering signal are exploited for IC, CoMP, and IN. By shaping a transmit beam using ZFBF, IA, or CoMP, the adjusted signal will be attenuated; a ZF-based filter can be adopted to nullify interference at the expense of degrading the desired signal power somewhat; and for IN, an interfering signal is duplicated to neutralize the interference at the cost of additional transmit power consumption. Moreover, ZFBF and ZF reception require multiple antennas or DoFs at the transmitter (Tx) and the receiver (Rx), respectively, and for IA, both ends of the communication link should be equipped with multiple antennas. The DoF requirements of these methods are determined by the signal dimensions, i.e., for ZFBF and ZF reception, each interfering signal component consumes one DoF, whereas for IA, at least one additional DoF should be provided to place the aligned interference. With IN, since interference(s) can be neutralized over the air, no additional receiver-side DoF is required to cancel interference, thus becoming free from the aforementioned limitations of ZF reception and IA.

TABLE I
COMPARISON OF IM METHODS

Feature \ Method	ZFBF	ZF	CoMP	IC	IA	IN	IS
Tx beam adjustment	○	×	○	×	○	×	×
Rx beam adjustment	×	○	×	×	×	×	×
Signal attenuation	○	○	○	×	○	×	×
Tx power cost	×	×	×	×	×	○	○
Tx side CSI exchange	○	×	○	×	○	○	○
Tx side data exchange	×	×	○	×	×	○	○
Rx side CSI exchange	×	○	×	○	×	×	×
Rx side data exchange	×	×	×	○	×	×	×
Tx side multi-antenna	○	×	○	×	○	○	○
Rx side multi-antenna	×	○	×	×	○	×	○
Symbol-level synchrony	×	×	○	○	×	○	○

Table I compares some signal-processing-based IM, where the symbols ○ and × indicate having and not having the corresponding feature, respectively. Tx beam indicates data transmission from various sources to their corresponding receivers. Rx beam means the direction of the receive filter's main lobe. Either transmitter or receiver beam adjustment will cause effective signal power loss. Tx/Rx-side CSI exchange indicates that the transmitter/receiver needs to acquire CSI from all Rxs/Txs, including intended and unintended Rxs/Txs, to itself. In practice, ZFBF and IA are implemented at the interfering transmitter, ZF is at the interfered receiver, CoMP and IC are realized cooperatively at the transmitter and receiver, respectively. When the interfering Tx is unwilling to perform IM, or collaboration between the interferer and the interfered transmission-pair cannot be established, all methods based on such collaboration will not be applicable.

The above discussion implies the need for a new solution to the interference problem despite the numerous IM schemes proposed thus far. Unlike those methods requiring implementation at either the interfering transmitter (for IA and ZFBF) or the interfered receiver (for ZF), we need the interfered Tx-side IM for the following reasons. First, due to the equal or higher priority of interfering transmission over the interfered transmission, the interferer may not be amenable to implementing IM, especially when it incurs some performance loss. For example, in a heterogeneous cellular network (HCN) where small cells are deployed on top of a macrocell to improve the capacity and coverage of existing cellular systems, the macro base station (STA) may interfere with small cell users.

[1]Since many practical systems are equipped with multiple antennas which has been known to greatly increase the degrees of freedom (DoFs) of communication systems [15], in this article we consider the realization of IA in multiantenna systems without requiring symbol extensions over very large number of time-frequency dimensions [16].

Due to the small cells' subordinate nature,[2] it is not practical to modify macrocell's transmissions for the interfered small cell users. Second, in some communication scenarios, such as a downlink transmission, acquiring information for IM (e.g., interferer identification) is always difficult or even impossible for the interfered receiver, especially when there are multiple interferers. So, in the above situations, the approaches listed in Table I (except for IN) are not applicable, and hence a new IM method is called for. We therefore focus on two aspects—the available information we can utilize and the cost of IM—in the development of novel IM. As shown in Table I, most existing methods exploit CSI while ignoring the data information that interference signal carries. Although IN is an interfered transmitter-based IM implementation which makes use of the interferer's data information, to the best of our knowledge, no existing IN schemes account for the power cost. That is, under a transmit power constraint, the more power consumed for IN, the less available for the intended signal's transmission. Especially when interference at the interfered Rx is relatively strong, there might not be sufficient power to generate a required neutralizing signal, thus making IN infeasible. The features of the proposed IS is similar to that of IN except for the multiantenna requirement at the receiver side. Here, it should be noticed that IN can neutralize interference without requiring multiple antennas at the Rx side, however, when there are multiple, say L, desired signals to be recovered, the receiver should be equipped at least L antennas so as to spatially distinguish these desired transmissions simultaneously. The details can be seen in the following sections.

By recognizing that interference can be not only neutralized but also steered in a particular direction, we first propose a novel IM method, called *interference steering* (IS). With IS, a duplicated interfering signal is generated to modify the spatial feature of the original interference observed by the interfered receiver, thus enabling interference-free data transmission. Then, we discuss the application of IS to an enterprise wireless local area network (WLAN), which has become a pervasive and essential part of our professional life, and will be increasingly important in the future IoT.

The main contributions of this article are twofold.

1) Proposal of a novel IM scheme called IS to provide a new insight for the design of IoT. By generating a steering signal, the original interference imposed on the interfered receiver is steered to the orthogonal direction with respect to the desired signal, hence achieving interference-free transmission. IS consumes less power than IN but requires an additional DoF at the interfered Rx. Moreover, IS can also subsume IN as a special case, thus becoming more general.
2) Discussion of the application of IS in an enterprise WLAN-based IoT scenario where the same frequency band is reused by adjacent BSSs with overlapping areas. A random network topology and arbitrary number of interferences are considered. With the proposed mechanism, interference to cell-edge users can be mitigated, allowing nearby APs to transmit to their associated STAs on the same channel simultaneously and hence improving the system's SE.

[2]Small cells are employed to assist macrocell to improve its service, while interfering Tx in macrocell does not necessarily adjust its transmission, or sacrifice its communication performance to avoid disturbance to interfered Rx in the small cell.

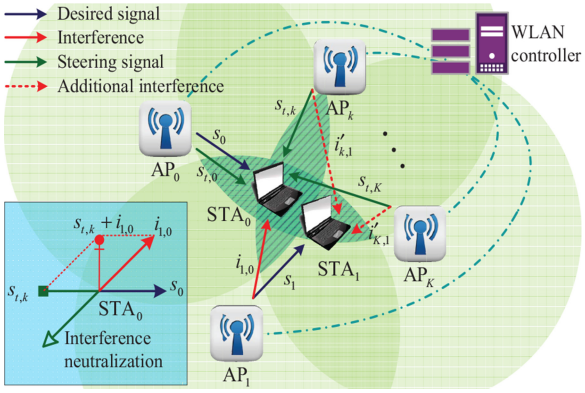

Fig. 1. Typical interference scenario in IoT.

The rest of this article is organized as follows. Section II describes the system model, while Section III presents the design of IS. In Section IV, the application of IS in enterprise WLAN is detailed. Section V evaluates the proposed mechanism. Finally, Section VI concludes this article.

Throughout this article, we use the following notations. The set of complex numbers is denoted as $\mathbb{C}$, while vectors and matrices are represented by bold lower-case and upper-case letters, respectively. Let $\mathbf{X}^H$, $\mathbf{X}^{\mathrm{T}}$ and $\mathbf{X}^{-1}$ denote the Hermitian, transpose and inverse of matrix $\mathbf{X}$. $\|\cdot\|$ indicates the Euclidean norm. $E(\cdot)$ denotes statistical expectation. $\langle \mathbf{a}, \mathbf{b} \rangle$ represents the inner product of two vectors.

II. System Model

Consider downlink communication in an infrastructure-based enterprise WLAN in which coverage areas of APs often overlap. For example, approximately 15% more APs (resulting in overlapping coverage) are required for wireless voice communications so as to achieve an acceptable reception power level [23]. Although data-only communications may not require such a large amount of overlap, in order to achieve seamless coverage, coverage overlap is inevitable. For example, Fig. 1 shows K adjacent BSSs with overlapping areas. All APs are assumed to have the same transmit power, P_T, and connected to a central WLAN controller so that downlink transmissions from APs to their clients/STAs are synchronized. Although multiple STAs may be in the coverage area of an AP, only one STA is served at a time by its associated AP via one frequency channel and each STA is associated with one AP at a time. For clarity of presentation, we show only two edge STAs: STA$_0$ is associated with AP$_0$ and STA$_1$ with AP$_1$. We assume APs and STAs each are equipped with N_t and N_r antennas, respectively. Since mobile STAs/devices are subject to more severe restrictions, such as cost and hardware than an AP, we assume $N_t \geq N_r > 1$. $\mathbf{H}_{mn} \in \mathbb{C}^{N_r \times N_t}$ denotes the spatial channel from AP$_m$ to STA$_n$. We employ a spatially uncorrelated Rayleigh flat fading channel model so that

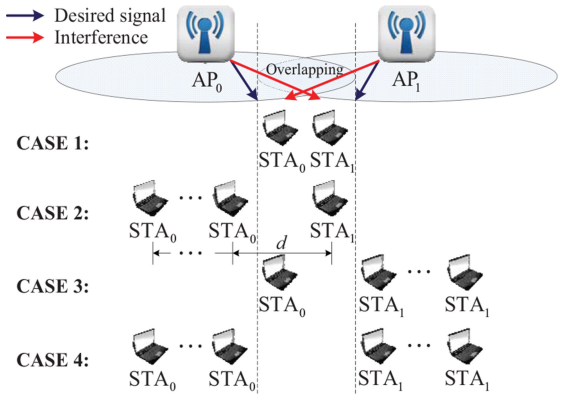

Fig. 2. Interference scenarios.

the elements of $\mathbf{H}_{mn}$ are modeled as independent and identically distributed zero-mean unit-variance complex Gaussian random variables. All users experience block fading, i.e., channel parameters in a block consisting of several successive transmission cycles remain constant in the block and vary randomly between blocks. Let s_m, $m \in \{1, \ldots, K\}$, be the desired signal from AP_m to its currently serving client STA_m, and $i_{m,n}$ ($n \in \{1, \ldots, K\}$) be the interference from AP_m to STA_n. $s_{t,m}$ is the steering signal generated by AP_m, while $i'_{m,n}$ is the additional interference caused by the steering signal $s_{t,m}$ to STA_n.

According to the existing IEEE 802.11 protocols, a STA scan RF channels to search for beacons advertising the presence of nearby APs. When a radio receives a beacon frame, it acquires information about the capability and configuration of the corresponding network, and then lists eligible APs. Based on the number of available APs in the list, the STA determines whether it is an edge-user[3] or not. The STA also estimates CSI based on the received null data packet (NDP) announcements from nearby APs [24]. In this system model, APs with overlapping areas should be scheduled by the central controller so that their NDP transmissions are serialized (to avoid collision). By analyzing the transmitter address field [25] in the NDP announcement, the STA can differentiate CSI from different APs. In general, a nonedge STA estimates and then reports CSI to its associated AP, while an edge-STA forms CSI from its associated AP as well as adjacent APs as a vector and sends the vector to its associated AP. The AP then delivers the CSI or CSI vector to the central controller.

Based on WLAN protocols, two adjacent BSSs contend for the same channel and cannot operate on the same channel simultaneously. However, for the purpose of SE enhancement, we may reuse spectrum more aggressively with effective IM. In such a case, co-channel interference (CCI) may occur, and a STA should thus be able to detect collision caused by CCI, i.e., distinguishing collision from fading individually [26] or cooperatively [27] with its associated AP. Fig. 2 illustrates common interference scenarios in WLAN. The figure shows downlink transmissions from AP_0 to STA_0 and from AP_1 to STA_1, initiate at time t_0 and t_1, respectively. This simplified discussion can be readily extended to the case of more APs and STAs as in real WLAN (see Sections III and IV). Without loss of generality, we let $t_1 \geq t_0$. Both AP and STA follow the listen-before-talk (LBT) rule, and channel reciprocity holds, i.e., if an AP can detect signal from an unassociated STA, its transmission signal will interfere with the STA's reception. Let d be the distance between STA_0 and STA_1. For simplicity, we assume inter-AP distance is large enough for APs to be unable to hear each other.

Let us consider the downlink transmissions from AP_0 to STA_0 and from AP_1 to STA_1 as an example that initiates transmission at time t_0 and t_1, respectively, and without loss of generality, we investigate the channel occupancy status observed by BSS_1 and use a general expression $[\text{STA}_0 \rightarrow \text{AP}_1, \text{AP}_0 \rightarrow \text{STA}_1]$ to represent the reachability between unassociated AP–STA pairs. For example, if AP_1 overhears STA_0, then the first bit in the above expression is 1 else 0. Since the reachability between STAs does not affect the downlink interference, the link $\text{STA}_0 \rightarrow \text{STA}_1$ is omitted. This simplified discussion can be readily extended to the case of more APs and STAs as in real WLAN (see Sections III and IV). We let $t_1 \geq t_0$. Both AP and STA follow the LBT rule, and channel reciprocity holds, i.e., if an AP can detect signal from an unassociated STA, its transmission signal will interfere with the STA's reception. For simplicity, we assume inter-AP distance is large enough for APs to ignore signals from each other. So, the reachability in case 1 of Fig. 2 is [1, 1], i.e., mutual interference occurs between two adjacent BSSs. We can simply block one of the transmissions or employ CoMP [13] to serve two STAs with both APs simultaneously, but CoMP requires modification of the interferer's transmission. As for the second situation, the reachability status is [0, 1], and hence AP_1 is allowed to initiate its transmission to STA_1 by employing an effective IM method to protect STA_1's reception. In case 3, the reachability status is $[1, 0]$. Since STA_0 is not associated with AP_1 and all BSSs are equal, AP_1 can transmit data to STA_1 regardless of the ongoing transmission from AP_0 to STA_0. Then, IM should be employed to guarantee STA_0's reception. CoMP is not applicable for cases 2 and 3, since not all STAs can hear from both APs. If we do not allow AP_1 to transmit to STA_1, an activated edge-STA will block transmissions on the same frequency channel in all its adjacent BSSs whose AP/STA is exposed to the interferer's signal radiation. This is undesirable for the network's requirement of high SE and system capacity. In the last situation, the reachability status is $[0, 0]$, so two interference-free transmissions can be established concurrently. Based on the above discussion, we focus on IM for cases 2 and 3, i.e., edge-STA in case of asymmetric interference. AP_1 and STA_0 act as the interfering transmitter and the interfered receiver, and STA_1 and AP_0, corresponding to the interfering Tx and interfered Rx, respectively, are termed without ambiguity as the interfering transmitter and the interfered receiver in the following discussion.

Since a STA is capable of detecting collision, upon sensing a conflict, the interfered STA reports to its associated AP, the latter (interfered Tx) asks the WLAN controller for assistance. The controller checks its database and finds a solution for the

[3]We use the term *edge* to indicate the status of a STA that can hear from more than one AP, rather than the geographical location of the STA.

requestor. The above procedure is in accordance with the centralized management framework proposed in 5G [2], where a high-level node manages all the information. Specifically, the controller maintains the association status between the corresponding APs and STAs, the transmitting status of each AP, and the data information to be transmitted. By utilizing such information, an IS solution can be obtained (see Section IV for details). To limit the system overhead, only edge-STAs can ask their associated APs for IM.

One should note that although we take WLAN as an example to design our mechanism, our scheme is still applicable to other types of networks in IoT as long as they are featured as: 1) direct/indirect[4] collaboration between the interfering Tx and interfered Tx is available and 2) the interference topology is asymmetrics.

III. Design of Interference Steering

We present the signal processing procedure of IS by exploiting both CSI with respect to and data carried in the interference(s). IS generates a steering signal to modify the interference's spatial feature, so that the original interference is steered to the orthogonal direction of the desired signal observed by the interfered receiver. In what follows, we first describe the basic design in terms of a single interference and then discuss a multi-interference scenario and cooperative IS.

A. Signal Processing of IS

We assume beamforming (BF) is employed for each downlink communication. As shown in Fig. 1, consider the transmission from AP_0 to STA_0 as an example that is corrupted by the signal sent from AP_1; the received signal at STA_0 with IS can be expressed as

$$\mathbf{y}_0 = \sqrt{P_T - P_0^{s_t}}\mathbf{H}_0\mathbf{p}_0 x_0 + \sqrt{P_T - P_1^{s_t}}\mathbf{H}_{10}\mathbf{p}_1 x_1 + \sqrt{P_k^{s_t}}\mathbf{H}_{k0}\mathbf{p}_k^{s_t} x_k^{s_t} + \mathbf{z}_0. \quad (1)$$

The first three items on the right-hand side (RHS) of (1) denote the desired signal from AP_0, interference from AP_1, and steering signal from AP_k where $k \in \{0, 1, \ldots, K\}$, respectively. $\mathbf{z}_0$ is an additive white Gaussian noise (AWGN) vector whose elements have zero mean and variance σ_n^2. Recall that $\mathbf{H}_{mn}$ represents the channel matrix from AP_m to STA_n. When $m = n$, we simply use one-letter subscript for conciseness. x_0 and x_1 are data symbols sent from AP_0 and AP_1, respectively. $E(\|x_0\|^2) = E(\|x_1\|^2) = 1$ holds. Since there is only one interference, data information carried by the steering signal is $x_k^{s_t} = x_1$. Theoretically, either AP_0, AP_1 or AP_k where $k \in \{2, \ldots, K\}$ can perform IS. Therefore, we use $P_0^{s_t}$, $P_1^{s_t}$, and $P_k^{s_t}$ to denote the transmit power cost for IS at AP_0, AP_1, and AP_k, respectively. $\mathbf{p}_0$ and $\mathbf{p}_1$ are the precoding vectors for x_0 and x_1 at AP_0 and AP_1, whereas $\mathbf{p}_k^{s_t}$ ($k \in \{0, \ldots, K\}$) is the precoder for steering signal at AP_k. When AP_0 (or AP_1) performs IS, $P_1^{s_t}$ (or $P_0^{s_t}$) and $P_k^{s_t}$ ($k \in \{2, \ldots, K\}$) become 0. Otherwise, when AP_k generates the steering signal, we have $P_0^{s_t} = P_1^{s_t} = 0$. We adopt the singular value decomposition (SVD)-based BF transmission, i.e., applying SVD to $\mathbf{H}_m$ to obtain $\mathbf{H}_m = \mathbf{U}_m\mathbf{D}_m\mathbf{V}_m^H$ and employing $\mathbf{p}_m = \mathbf{v}_m^{(1)}$ where $\mathbf{v}_m^{(1)}$ represents the principal column vector of $\mathbf{V}_m$. We can simply use $\mathbf{u}_m^{(1)}$ as the filter vector, where $\mathbf{u}_m^{(1)}$ is the first column vector of $\mathbf{U}_m$. Then, the estimated signal $\bar{y}_m = [\mathbf{u}_m^{(1)}]^H\mathbf{y}_m$.

[4]*Direct collaboration* refers to direct information exchange between transmitters, whereas *indirect* indicates that the cooperation is achieved via a central control node, e.g., WLAN controller in Fig. 1.

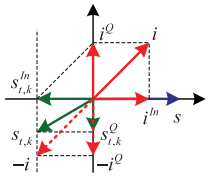

Fig. 3. Illustration of IS.

IS is designed as follows. We first define the directions of desired signal and original interference combined with steering signal as

$$\mathbf{d}_s = \frac{\mathbf{H}_0\mathbf{p}_0}{\|\mathbf{H}_0\mathbf{p}_0\|} \quad (2)$$

and

$$\mathbf{d}_{i+s_{t,k}} = \frac{\sqrt{P_T}\mathbf{H}_{10}\mathbf{p}_1 + \sqrt{P_k^{s_t}}\mathbf{H}_{k0}\mathbf{p}_k^{s_t}}{\left\|\sqrt{P_T}\mathbf{H}_{10}\mathbf{p}_1 + \sqrt{P_k^{s_t}}\mathbf{H}_{k0}\mathbf{p}_k^{s_t}\right\|} \quad (3)$$

respectively. Then, by letting $\langle \mathbf{d}_s, \mathbf{d}_{i+s_{t,k}} \rangle = 0$, the original interference can be steered to the orthogonal direction with respect to the desired signal by the steering signal, s_t.

Since both interference and steering signal, denoted by i and $s_{t,k}$, respectively, can be decomposed into an in-phase component and a quadrature component, denoted by superscripts *In* and Q, respectively, with respect to $\mathbf{d}_s$, i.e., $i = i^{\text{In}} + i^Q$ and $s_{t,k} = s_{t,k}^{\text{In}} + s_{t,k}^Q$, when $s_{t,k}^{\text{In}} = -i^{\text{In}}$, IS is realized. Fig. 3 illustrates the basic principle of IS. A 2-D representation is employed for readability. The vectors in the figure indicate the spatial signals.

It can be easily seen that given $s_{t,k}^{\text{In}} = -i^{\text{In}}$, interference energy imposed on the desired transmission is countered. As $s_{t,k}^Q$ approaches $-i^Q$, $s_{t,k}$ tends to $-i$, i.e., IN is achieved. Since the length of vector indicates the strength of signal, when $s_{t,k}^Q = 0$, we have $s_{t,k} = s_{t,k}^{\text{In}}$, and obtain an IS solution with minimum power overhead.

Based on the above discussion, we take the communication scenario depicted in Fig. 1 as an example. A general expression of IS implementation is then given as

$$\begin{cases} \mathbf{p}_k^{s_t} = \mathbf{H}_{k0}^{-1}\left[s_{t,k}^{\text{In}} + s_{t,k}^Q\right] \Big/ \left\|\mathbf{H}_{k0}^{-1}\left[s_{t,k}^{\text{In}} + s_{t,k}^Q\right]\right\| \\ P_k^{s_t} = \left\|\mathbf{H}_{k0}^{-1}[s_{t,k}^{\text{In}} + s_{t,k}^Q]\right\|^2 \end{cases} \quad (4)$$

where $s_{t,k}^{\text{In}} = -i^{\text{In}} = -\sqrt{P_T}\mathbf{P}\mathbf{H}_{10}\mathbf{p}_1$ and $\mathbf{P} = \mathbf{d}_s(\mathbf{d}_s^H\mathbf{d}_s)^{-1}\mathbf{d}_s^H$ denotes projection matrix. When $s_{t,k}^Q = -\sqrt{P_T}\mathbf{H}_{10}\mathbf{p}_1 + \sqrt{P_T}\mathbf{P}\mathbf{H}_{10}\mathbf{p}_1$, we have $s_{t,k} = -i$ and IS becomes IN. Then, (4) can be rewritten as

$$\begin{cases} \mathbf{p}_k^{n_e} = -\mathbf{H}_{k0}^{-1}\mathbf{H}_{10}\mathbf{p}_1 \Big/ \left\|\mathbf{H}_{k0}^{-1}\mathbf{H}_{10}\mathbf{p}_1\right\| \\ P_k^{n_e} = \left\|\mathbf{H}_{k0}^{-1}\mathbf{H}_{10}\mathbf{p}_1\right\|^2. \end{cases} \quad (5)$$

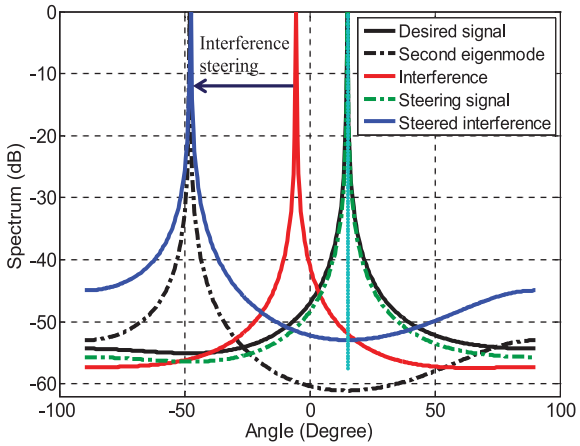

Fig. 4. Spatial spectrums of different signals.

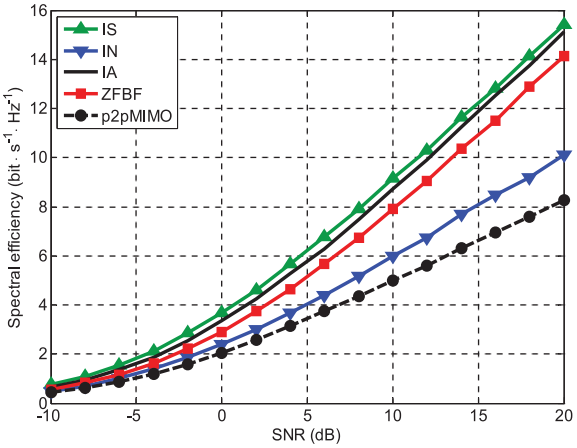

Fig. 5. Average system SE with different IM methods.

Note that the above results are obtained under $N_t = N_r$; when $N_t > N_r$, the inverse of $\mathbf{H}_{k0}$ should be replaced by its Moore–Penrose pseudo inverse. One can now easily see that IS subsumes IN as a special case, making IS more general. Considering the power overhead, we limit the sum of $P_k^{s_t}$ and power for the desired signal's transmission to a fixed value P_T. Moreover, only $s_{t,k}^{Q} = 0$ is considered in our current design.

Fig. 4 plots spatial spectra of various signals to show the feasibility of IS where $N_t = N_r = 2$ and the desired and interference signals are randomly generated. The center frequency of input signal is $f_0 = 2.4$ GHz, the antenna-element spacing is half of the signal wavelength, and the SNR of each signal is 20 dB. We first employ the multiple signal classification (MUSIC) algorithm to estimate direction of arrival (DoA) of each signal. Then, we reconstruct the spatial spectrum of signal components observed at the receiver. For ease of comparison, we also plot signal transmission via the second eigenmode which is orthogonal to the desired signal utilizing the principal eigenmode. Fig. 4 shows that the steering signal moves the interference's DoA to be the same as the DoA of signal using the second eigenmode. Moreover, the lowest point of the steered interference overlaps with the peak of the desired signal. That is, the desired transmission has become interference-free.

It should be noted that generating steering signal consumes transmit power at the AP, thus given a fixed power budget, the power used for the desired signal's transmission reduces as the power overhead of IS increases. Therefore, the allocation of transmitter's power to the IS and desired signal's transmission can be optimized to further enhance IS's performance [28].

B. Comparison of IS and Other Transmitter-Based Methods

So far, we have presented the basic signal processing of IS. One may think IS similar to some existing IM methods, such as IA, ZFBF, CoMP, IN, etc., but it is not. Basically, all of IA, ZFBF, and CoMP require modifications at the interferer, so that the transmission from an interfering transmitter to its intended receiver is attenuated. In case of CoMP, the user is served by multiple APs cooperatively. IN and IS are interfered transmitter-side implementations which are suitable only when the interferer is willing to sacrifice, i.e., some performance loss with respect to the interfering transmission-pair will be incurred when the interferer realizes IM, as is usually the case. Compared to IN, IS focuses on canceling only the effective part of the interference, thus becoming more power-efficient. However, it costs one DoF at receiver, just as IA. Compared to IA, the main difference of IS designed in this article is that IA needs the attenuation/sacrifice of interfering user-pairs' transmission whereas IS does not.

Without specifications, the following simulation results in this article are under $N_t = N_r = 2$. However, the same conclusion can be drawn with various antenna settings. For space limitation, we omit the results for other N_t and N_r values. Fig. 5 comparatively evaluates the achievable system SE of IA, ZFBF, IN, and IS by using MATLAB simulation and with the consideration of two communication pairs ($K = 2$)—from AP_0 to STA_0 and from AP_1 to STA_1. AP_1 interferes with STA_0. Note that IA and ZFBF are implemented at AP_1, incurring performance loss to the transmission from AP_1 to STA_1. As for ZFBF, since N_t should be no less than the total number of receiving antennas across all receivers, we let $N_r = 1$. With the other three methods, $N_t = N_r = 2$. IN and IS are carried out by AP_0, when their power overheads, $P_0^{n_e}$ and $P_0^{s_t}$, exceed the power budget of an AP, e.g., P_T, we simply regard the interfered transmission's SE as 0. In the figure, SE of an interference-free point-to-point MIMO (p2pMIMO) transmission employing BF is also plotted as a reference. IS is shown to yield the best system SE (SE of $K = 2$ transmissions). Since $N_r = 1$, the SE performance of ZFBF is inferior to that of IS and IA. System SE of IN is close to that of p2pMIMO, so SE of the transmission pair using IN is inferred to be very low. It should be noted that due to the randomness of wireless channels, IS may incur more cost compared to IA, thus outputting lower SE under some channel conditions. However, as shown in the figure, the system SE of IS is statistically higher than that of IA.

C. Multi-Interference Processing

In the above discussion, only one interferer is considered. In practical use, an IoT device may be interfered by multiple

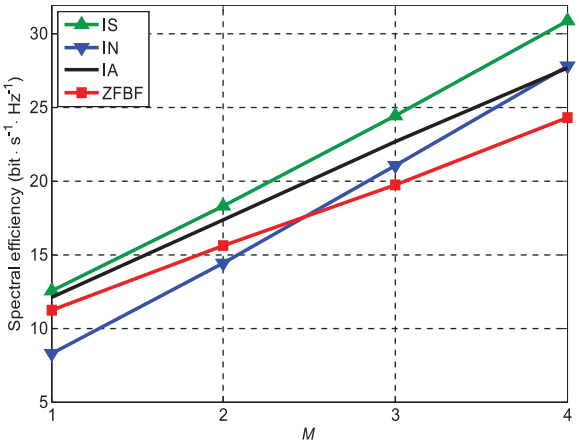

Fig. 6. System SE under $M \in \{1, 2, 3, 4\}$ and SNR=15 dB.

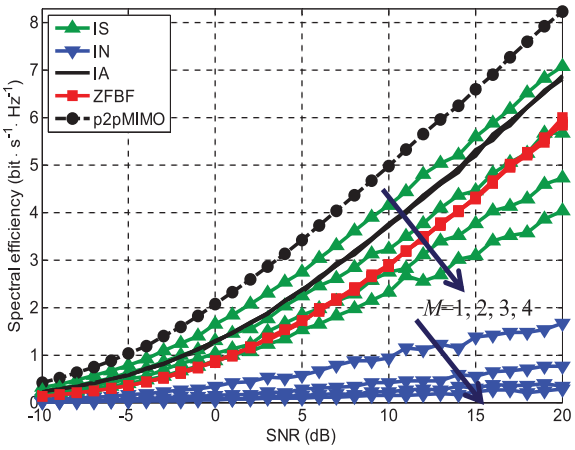

Fig. 7. SE of a single transmission pair under $M \in \{1, 2, 3, 4\}$.

nearby transmitters. We still take WLAN as an example. When an interfered STA suffers from multiple APs, its associated AP asks the WLAN controller for assistance. The latter is able to check these interference components, combine them together, and then calculate an IS solution in terms of this combined interference [29]. In other words, multiple independent interferences are not treated individually but as a whole (after combining them), and hence the dimension of interference is reduced to 1. In the case of multi-interference, (1) can be rewritten as

$$\mathbf{y}_0 = \sqrt{P_T - P_0^{s_t}}\mathbf{H}_0\mathbf{p}_0 x_0 + \sum_{m\in\{1,\ldots,M\}} \sqrt{P_T - P_m^{s_t}}\mathbf{H}_{m0}\mathbf{p}_m x_m + \sqrt{P_k^{s_t}}\mathbf{H}_{k0}\mathbf{p}_k^{s_t} x_k^{s_t} + \mathbf{z}_0. \tag{6}$$

m and M are the index and the total number of interferences, respectively. Transmission from AP_0 to STA_0 is interfered with by the other $M = K-1$ transmissions. $x_k^{s_t}$ is dependent on the combination of all interferences. When AP_0 (or AP_m where $m \in \{1, \ldots, M\}$) performs IS, $P_m^{s_t}$ (or $P_0^{s_t}$) and $P_k^{s_t}$ where $k \in \{M+1, \ldots, K\}$ become 0. Otherwise, when AP_k ($k \in \{M+1, \ldots, K\}$) generates steering signal, we have $P_0^{s_t} = P_m^{s_t} = 0$. The detailed extension of IS to the multi-interference situation can be found in [30].

As in Fig. 6, MATLAB simulation is employed to evaluate the overall SE of $K = M+1$ transmissions of which M are interferers and 1 is the interfered, for different IM methods. For simplicity, we assume no interference between any two interferers. As shown in Fig. 6, the system SE improves as M increases. With IA and ZFBF, the interfering Tx conducts IM, thus degrading all transmissions from the interfering transmitters to their intended receivers. In case of IS and IN, AP_0 performs the IM; only the interfered transmission is affected. However, IS incurs much less power cost than IN, and hence yields higher SE than IN under a transmit power constraint. Thus, IS is shown to provide the best performance, while IN's SE gradually approaches IA's and exceeds ZFBF's as M increases.

We use $r_{s_0}^{\mathcal{M}}$, $r_{s_m}^{\mathcal{M}}$, and $R_{\text{sys}}^{\mathcal{M}}$ to denote the average SE of the interfered AP_0's transmission to STA_0, the interferer's own transmission from AP_m to STA_m, where $m \in \{1, \ldots, K-1\}$, and the system employing $\mathcal{M}$ as the IM method, respectively. r_{BF} is the SE of p2pMIMO with BF. Without loss of generality, we let the interfered AP_0 carry out IN or IS. Then, the average system SE of IS, IN, IA, and ZFBF with M interferers can be calculated as

$$R_{\text{sys}}^{\text{IS}} = r_{s_0}^{\text{IS}} + M r_{\text{BF}} \tag{7}$$

$$R_{\text{sys}}^{\text{IN}} = r_{s_0}^{\text{IN}} + M r_{\text{BF}} \tag{8}$$

$$R_{\text{sys}}^{\text{IA}} = r_{\text{BF}} + \sum_{m}^{M} r_{s_m}^{\text{IA}} \tag{9}$$

$$R_{\text{sys}}^{\text{ZFBF}} = r_{\text{BF}} + \sum_{m}^{M} r_{s_m}^{\text{ZFBF}}. \tag{10}$$

For example, when IS or IN is employed, the SE of the interfered transmission is $r_{s_0}^{\text{IS}}$ or $r_{s_0}^{\text{IN}}$, whereas for the other transmissions, SE is calculated in terms of p2pMIMO. That is, although $r_{s_0}^{\text{IS}}$ and $r_{s_0}^{\text{IN}}$ decreases as M grows, $R_{\text{sys}}^{\text{IS}}$ and $R_{\text{sys}}^{\text{IN}}$ are dominated by Mr_{BF} which grows linearly with M, thus enhancing the system SE. When IN or IS is implemented at AP_k where $k \in \{1, \ldots, M\}$, the AP_0's transmission to STA_0 is free of interference, and hence its SE is equal to r_{BF}. We then have

$$R_{\text{sys}}^{\text{IS}} = r_{s_k}^{\text{IS}} + M r_{\text{BF}} \tag{11}$$

and

$$R_{\text{sys}}^{\text{IN}} = r_{s_k}^{\text{IN}} + M r_{\text{BF}}. \tag{12}$$

In the case of IA and ZFBF, the interfered transmission becomes free of interference, and hence its SE is equal to r_{BF}. Since $r_{s_m}^{\text{IA}} < r_{\text{BF}}$ and $r_{s_m}^{\text{ZFBF}} < r_{\text{BF}}$, protection of STA_0 from the interference of AP_m ($m \in \{1, \ldots, M\}$) requires the sacrifice of SE of all the interfering transmissions.

Fig. 7 shows the SE of a single transmission pair for different IM methods. AP_0's transmission to STA_0 is interfered with by the other $M = K-1$ transmissions. Under IS and IN, we let AP_0 perform IM, and plot $r_{s_0}^{\text{IS}}$ and $r_{s_0}^{\text{IN}}$, while studying the SE of an arbitrary interfering transmission—i.e., $r_{s_m}^{\text{IA}}$ and $r_{s_m}^{\text{ZFBF}}$, $m \in \{1, \ldots, M\}$—under IA and ZFBF. Both $r_{s_0}^{\text{IS}}$ and $r_{s_0}^{\text{IN}}$ are shown to decrease as M increases. In the case of the

transmission pair with IA or ZFBF, there is no interference to it, thus making its SE independent of M. From Fig. 7, we can obtain the SE loss of one communication pair which implements an IM method by subtracting the SE of the corresponding method from that of p2pMIMO. With IS and IN, the interfered transmission suffers from some SE loss, whereas for ZFBF and IA, each interferer sacrifices its SE performance so as to avoid interference to the interfered receiver. As a result, for IS and IN, in order to guarantee the interfered transmission's performance, the number of interferences to a Rx, denoted by η (see Section V), should be limited.

D. No Need for Cooperative IS

Two types of IS are conceivable: cooperative and noncooperative. In case of the former, IS is performed by the interfering AP or the other adjacent AP that the interfered STA is not associated with, whereas the interfered AP generates the IS signal in the case of the latter. Note, however, both schemes require the collaboration, i.e., CSI and data sharing, between the AP performing IS and the interfering AP. We elaborate below why cooperative IS is not necessary from two aspects.

First, let us consider the performance of IS implemented by the interfered STA's nearby AP other than its associated AP and the interfering AP, i.e., AP_k ($k \in \{2, \ldots, K\}$). In this case, for ease of comparison we let the power of AP_k be P_T, and assume that the STA_k served by AP_k is free from interference while performing IS. Then, according to Fig. 1 and the design in Section III-A, the received SNR of STA_k where $k \in \{0, 2, \ldots, K\}$ is

$$\gamma_k = \left(P_T - P_k^{s_t}\right)\left[\lambda_k^{(1)}\right]^2/\sigma_n^2. \tag{13}$$

It can be easily seen from (13) that γ_k is determined by the power cost of IS. If IS is carried out by AP_0, $P_0^{s_t}$ is given by $P_0^{s_t} = P_T\|\mathbf{H}_0^{-1}\mathbf{P}\mathbf{H}_{10}\mathbf{p}_1\|^2$. Substituting $\mathbf{P} = \mathbf{d}_s(\mathbf{d}_s^H\mathbf{d}_s)^{-1}\mathbf{d}_s^H$ into $P_0^{s_t}$, we can obtain the power overhead of noncooperative IS as

$$P_0^{s_t} = P_T\frac{1}{\|\mathbf{H}_0\mathbf{p}_0\|^2}\left\|\mathbf{H}_0^{-1}\mathbf{H}_0\mathbf{p}_0\right\|^2\psi = P_T\frac{1}{\|\mathbf{H}_0\mathbf{p}_0\|^2}\psi \tag{14}$$

where $\psi = \|(\mathbf{d}_s^H\mathbf{d}_s)^{-1}\mathbf{d}_s^H\mathbf{H}_{10}\mathbf{p}_1\|^2$. Similarly, when AP_k implements IS for STA_0, where $k \in \{2, \ldots, K\}$, the power consumption of cooperative IS is

$$P_k^{s_t} = P_T\frac{1}{\|\mathbf{H}_0\mathbf{p}_0\|^2}\left\|\mathbf{H}_{k0}^{-1}\mathbf{H}_0\mathbf{p}_0\right\|^2\psi. \tag{15}$$

We use MATLAB simulation to obtain the probability that $P_0^{s_t}$ is less than $P_k^{s_t}$ ($k \in \{2, \ldots, K\}$), or equivalently $\|\mathbf{H}_{k0}^{-1}\mathbf{H}_0\mathbf{p}_0\| < 1$, as shown in Fig. 8. Although the above derivation is based on the single-interference assumption, the results for multiple interferences can also be derived, as shown in the figure. Since IN is a special case of IS, the power overheads of noncooperative and cooperative IN, denoted by $P_0^{n_e}$ and $P_k^{n_e}$ ($k \in \{2, \ldots, K\}$), respectively, are also studied. The probability of $P_0^{s_t} < P_k^{s_t}$ is notably higher than that of $P_0^{n_e} < P_k^{n_e}$, and both are independent of the number of interferences, M. This is because cooperative IS consumes more power than the noncooperative one, whereas for IN, the

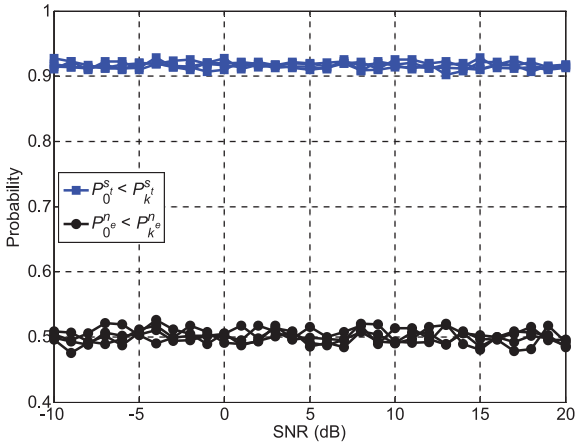

Fig. 8. Comparison of power cost under $M \in \{1, 2, 3, 4\}$.

power cost is statistically the same with or without collaboration. So, we conclude that IS should better be implemented at the interfered transmitter, whereas for IN, selective diversity gain can be obtained by adaptively choosing candidate Txs which are willing to assist the interfered Rx in IN. It should be noted that the above analysis ignores the effect of steering signal on STA_k for simplicity. In practical use, when AP_k ($k \in \{2, \ldots, K\}$) performs IS, the steering signal generated by AP_k will cause interference to AP_k's own transmission, thus deteriorating the system performance. This can further verify that the interfered AP is more suitable to perform IS.

Then, there may not exist strong motivation for the interfering AP to implement IS, since such an implementation will deteriorate its own transmission and there is not enough incentive to help the other AP's client. Take the communication scenario depicted in Fig. 1 as an example. If AP_1 carries out IS for STA_0, the received signal at STA_1 becomes

$$\mathbf{y}_1 = \sqrt{P_T - P_1^{s_t}}\mathbf{H}_1\mathbf{p}_1x_1 + \sqrt{P_1^{s_t}}\mathbf{H}_1\mathbf{p}_1^{s_t}x_1^{s_t} + \mathbf{z}_1 \tag{16}$$

where $x_1^{s_t} = x_1$. Therefore, the steering signal may contribute to or impair the transmission form AP_1 to STA_1. By employing $\mathbf{u}_1^{(1)}$ as the receive filter, and noting that the first two signal components on the RHS of (16) are neither in the same direction nor orthogonal, the effective received signal of STA_1 satisfies the following equation:

$$\alpha_1 = \left\|\left[\mathbf{u}_1^{(1)}\right]^H\left(\sqrt{P_T - P_1^{(s_t)}}\mathbf{H}_1\mathbf{p}_1 + \sqrt{P_1^{(s_t)}}\mathbf{H}_1\mathbf{p}_1^{s_t}\right)\right\|^2. \tag{17}$$

We define

$$\alpha_1^{(1)} = \left\|\left[\mathbf{u}_1^{(1)}\right]^H\sqrt{P_T - P_1^{(s_t)}}\mathbf{H}_1\mathbf{p}_1\right\|^2 \tag{18}$$

and

$$\alpha_1^{(2)} = \left\|\left[\mathbf{u}_1^{(1)}\right]^H\sqrt{P_1^{(s_t)}}\mathbf{H}_1\mathbf{p}_1^{s_t}\right\|^2 \tag{19}$$

which represent the components of desired transmission and steering signal sent from AP_1, respectively. Then, we plot α_1, $\alpha_1^{(1)}$, and $\alpha_1^{(2)}$ normalized by the noise power σ_n^2 in Fig. 9. We can see that the steering signal $\sqrt{P_1^{(s_t)}}\mathbf{H}_1\mathbf{p}_1^{s_t}x_1^{s_t}$ statistically

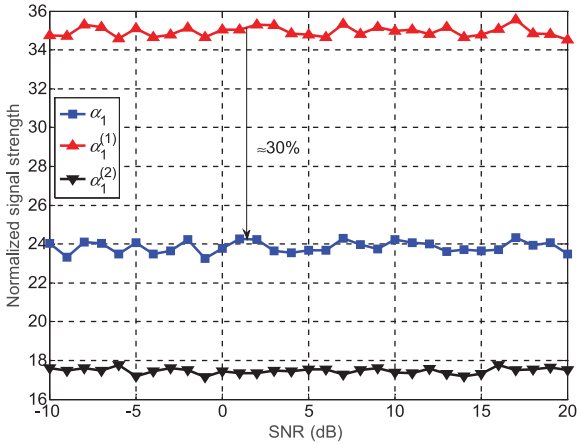

Fig. 9. Received signal strength at STA_1.

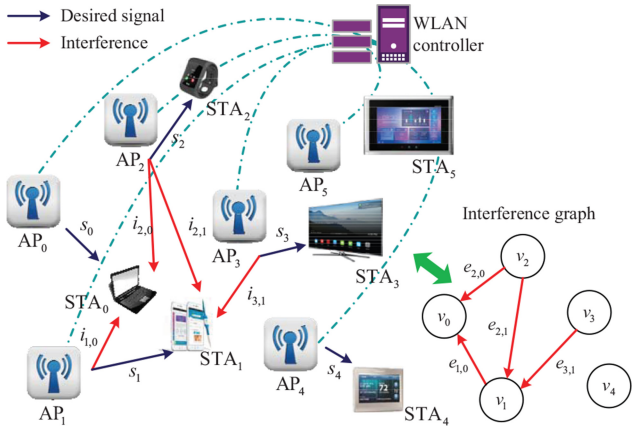

Fig. 10. Example IoT with multiple interferences and its interference graph.

weakens the desired signal component $\sqrt{P_T - P_1^{(s_t)}}\mathbf{H}_1\mathbf{p}_1 x_1$. Therefore, inequality $E(\alpha_1) < E[\alpha_1^{(1)}]$ holds. Similarly to the discussion about the implementation of IS by AP_k ($k \in \{2, \ldots, K\}$), we can conclude that realization of IS at AP_1 will lead to $P_0^{s_t}$ being statistically less than $P_1^{s_t}$. That is, performing IS at the interfering AP is not cost-effective.

In summary, it is preferable to employ AP_0 to implement IS rather than other AP_k where $k \neq 0$.

In the previous discussion, Fig. 8 has shown that $P_0^{s_t}$ is statistically lower than $P_k^{s_t}$ ($k \notin \{0, 1\}$) while Fig. 9 indicates that the interfering AP is not cost-effective in performing IS. Therefore, AP_0 is preferred to generate the steering signal. However, in practical use there is still a possibility that AP_k is more power-efficient in performing IS than AP_0 under certain channel realizations. So, adaptive selection of the proper AP for IS can theoretically further improve the interfered transmission's SE performance. However, for the following four reasons we omit such discussion. First, as abovementioned, there is little motivation for AP_k to realize IS for other transmission pair, let alone generating steering signal consumes AP_k's power which can be used for its own transmission. Second, according to the results given in Fig. 8, the probability that AP_0 is better than AP_k in performing IS is as high as 90%, therefore, it can be predicted that the improvement of interfered transmission's SE from adaptive selection of AP is marginal. Third, as Fig. 9 shows, generating steering signal may incur CCI among the transmissions from AP_1 to its serving STA, hence impairing the interfering transmission-pair's own performance, especially when there are multiple desired signals (acting as interferences to STA_0) sent from AP_1. Fourth, realizing adaptive selection of AP yields more computational complexity and signaling overhead. Therefore, letting the interfered AP perform IS is reasonable and easy to implement.

IV. Application of IS in IoT

In this section, we elaborate the application of IS in an enterprise WLAN-based IoT scenario. Fig. 10 shows an example network with $K = 6$ BSSs. However, our discussion can be extended to a general network with a random topology and arbitrary number of interferences. Since an AP can only serve one STA on a frequency channel at a time, other users with transmission demand will be moved to different channels. Without loss of generality, we use STA_m ($m \in \{0, \ldots, K-1\}$) to represent the current client served by AP_m. Since there are overlapping areas among adjacent BSSs and all BSSs reuse the same frequency channel, CCI should be well managed so that multiple interfering transmissions can be supported simultaneously. In the next two sections, we will first discuss the maintenance of information required for IS and use graph theory to analyze the interference relationship among multiple BSSs. We will then elaborate the realization of IS at different network entities.

A. Data Structure and Graph Analysis

In order to achieve IS, a proper data structure should be used for managing necessary network information. We adopt a *connection matrix* $\mathbf{C}$ and a *transmitting status vector* $\mathbf{T}$ for this purpose. $\mathbf{C}$ and $\mathbf{T}$ of the WLAN depicted in Fig. 10 are then expressed as

$$\mathbf{C} = \begin{bmatrix} 1 & 1 & 1 & 0 & 0 & 0 \\ 0 & 1 & 1 & 1 & 0 & 0 \\ 0 & 0 & 1 & 0 & 0 & 0 \\ 0 & 0 & 0 & 1 & 0 & 1 \\ 0 & 0 & 0 & 0 & 1 & 0 \\ 0 & 0 & 0 & 0 & 0 & 1 \end{bmatrix} \tag{20}$$

and

$$\mathbf{T} = [1\ 1\ 1\ 1\ 1\ 0]. \tag{21}$$

As shown in (20), if STA_n can (not) hear AP_m, then its connection status $\mathbf{C}(n+1, m+1) = 1(0)$. The principal diagonal elements of $\mathbf{C}$ are 1 due to the association between the corresponding APs and STAs. For example, STA_0 is associated with AP_0, and hence $\mathbf{C}(1, 1) = 1$. STA_0 can also hear adjacent nonassociated APs, say AP_1 and AP_2, then $\mathbf{C}(1, 2) = \mathbf{C}(1, 3) = 1$. In the case of STA_3, although AP_5 is not transmitting to STA_5, STA_3 is in the coverage of AP_5, and thus $\mathbf{C}(4, 5) = 1$. From (21), we can see that when AP_m

transmits to its associated client STA_m, the $(m+1)^{\text{th}}$ element of $\mathbf{T}$, $\mathbf{T}(m)$, is 1.

Both $\mathbf{C}$ and $\mathbf{T}$ are constructed based on the feedbacks from all APs and maintained by the WLAN controller. When a collision is detected and reported to an AP, the AP will inquire the central controller. Upon receiving the IM requirement, the controller performs the operation in (22) to obtain the *adjacency matrix*, or the *interference matrix*, represented by $\mathbf{A}$ as

$$\mathbf{A} = \text{diag}(\mathbf{T})(\mathbf{C} - \mathbf{I}) \tag{22}$$

where $\text{diag}(\mathbf{a})$ indicates the diagonalization of vector $\mathbf{a}$ and $\mathbf{I}$ is a $K \times K$ unit matrix. $\mathbf{A}$ specifies the interferences among all BSSs. For example, substituting (20) and (21) into (22), we can get

$$\mathbf{A} = \begin{bmatrix} 0 & 1 & 1 & 0 & 0 & 0 \\ 0 & 0 & 1 & 1 & 0 & 0 \\ 0 & 0 & 0 & 0 & 0 & 0 \\ 0 & 0 & 0 & 0 & 0 & 1 \\ 0 & 0 & 0 & 0 & 0 & 0 \\ 0 & 0 & 0 & 0 & 0 & 0 \end{bmatrix} \tag{23}$$

based on which an IS solution for the network can be calculated as discussed in the next section.

So far, the network's interference status is represented by $\mathbf{A}$. According to graph theory, an interference graph can also be employed to describe the interference relationship among BSSs. As shown in Fig. 10(bottom-right), each vertex denoted by v_m indicates a data transmission in a BSS. The directed edge $e_{m,n}$ represents the interference from vertex m to n. The weight of an edge could be the strength of interference to its destination. Since AP_5 is not in service, v_5 is not included in the graph.

Before delving into interference further, we first provide a theorem to show the feasibility characterization of IS. Then, the proof is given based on the discussion about some useful properties of the interference graph.

Theorem 1: A set of directed links are feasible for IS if and only if their interference graph is acyclic.

Proof: First, since we assume use of BF by all transmissions, the number of edges between two adjacent vertices is at most one. However, our design can be easily extended to the case where spatial multiplexing (SM) is used by the interferer and/or the interfered BSS. Such an extension does not affect the applicability of IS. On the one hand, when the interferer adopts SM, there exist multiple interference components, but since IS is designed based on the aggregated effect of interference, IS is achievable in the same way as in the single-interference case. On the other hand, when the interfered BSS employs SM, there will be multiple mutually orthogonal intended transmissions from the interfered AP to its recipient. Since each steering signal is in the opposite direction to the corresponding desired signal component, the steering signal for one spatial data stream will not interfere with the others and an IS solution for the STA receiving multiple desired streams is available.

Second, an AP cannot implement IS for more than one interfered STA simultaneously due to the nonorthogonality of transmissions to these STAs. For example, if an AP serves two clients both of which are interfered with by nearby AP(s), when the interfered AP generates a steering signal for one interfered user, additional interference (regarded as the side-effect of IS) will be incurred to the other interfered transmission, and vice versa, thus making IS unavailable.

Third, we do not advocate cooperative IS due to its higher power overhead than the noncooperative counterpart. In addition, an AP's assistance of another AP's client in achieving IS will incur additional interference to ongoing transmissions of its associated STA as well as nonassociated STAs in its coverage area. An IS solution that counts for assistant AP selection will be very difficult, or even impossible to obtain due to the increased computational complexity or because the problem may become nonconvergent. For example, when AP_k is employed for sending a steering signal $s_{t,k}$ to assist AP_0 in IS, as shown in Fig. 1, an additional interference $i'_{k,1}$ will be imposed on STA_1. If AP_1 adjusts its transmission to adapt to this interference, the interference from AP_1 to STA_0, i.e., $i_{1,0}$ varies, needing an updated steering signal from AP_k. Since the above process is nonconvergent, cooperative IS is unavailable in such a situation.

Fourth, recall that for the first case in Fig. 2, an interference cycle, i.e., mutual-interference between two BSSs, occurs, and then one transmission is blocked. When this situation is generalized to the multi-BSS ($K \geq 3$) scenario, similarly to the two-BSS case, we disallow cycles, i.e., if there is (are) cycle(s), then at least one vertex should be deleted so as to break cycle(s). This can be explained in terms of the side effects of IS, i.e., additional interference. Take a three-node cycle as an example in Fig. 10 where $e_{2,0}$ is replaced with $e_{0,2}$, forming a cycle with v_0, $e_{0,2}$, v_2, $e_{2,1}$, v_1, and $e_{1,0}$. Without loss of generality, we calculate an IS solution for v_0 first and then obtain $s_{t,0}$. Since $s_{t,0}$ introduces additional interference $i'_{0,2}$ to v_2, a steering signal for v_2 should be generated based on $i_{0,2} + i'_{0,2}$. Similarly, $s_{t,1}$ is calculated in terms of $i_{2,1} + i_{0,2} + i'_{0,2}$. In the end, $i'_{1,0}$ yielded by $s_{t,1}$ will lead to the recalculation of $s_{t,0}$ at v_0. This phenomenon is similar to a positive feedback that makes a stable IS solution unavailable in a network with interference cycles.

Based on the above discussion, Theorem 1 follows. ■

To be specific, in order to achieve IS, the original interference graph should be converted to a directed acyclic graph (DAG) [31]. Moreover, due to the randomness of networks, the interference graph may not be connected. Thus, given an interference graph, we should first check its connectivity. For each connected part, we employ a depth-first search (DFS) algorithm to detect cycles [31]. Considering the fact that each vertex represents a data transmission, we break a cycle by deleting a set of nodes according to the following two rules. First, remove as few vertices as possible. Second, if the first rule is met, the sum weight of the outgoing edges of the deleted node set should be maximized, i.e., remove the set of nodes generating the most interference. A brute-force search can be used to obtain such a set of nodes.

So far, we can obtain one or multiple DAGs, depending on the connectivity of the original interference graph. Then, an IS solution is calculated for each subgraph. Topological sorting [31] is used to determine the order of vertices that IS is computed for. Before detailing the application of this

algorithm in the next section, we introduce one definition and two properties of the DAG of our interest as follows.

Definition 1: For a vertex, the number of tail ends adjacent to a vertex is called the *indegree* of the vertex and the number of head ends adjacent to a vertex is its *outdegree*.

Property 1: Every acyclic graph contains at least one vertex with zero indegree; otherwise, there is a cycle.

Proof: The proof can be found in [32]. ■

Property 2: The interference graph remains unchanged with noncooperative IS.

Proof: Note that each vertex represents a data transmission and the transmission range of a steering signal is the same as its data signal. Given an interference graph, if there is an edge, say $e_{m,n}$, between two vertices, and AP_m generates steering signal $s_{t,m}$ for its client, then the interference $i'_{m,n}$ caused by $s_{t,m}$ in addition to the original interference $i_{m,n}$ will be incurred to STA_n being served by AP_n; if there is no edge between v_m and v_n, after AP_m implements IS, STA_n receives nothing from AP_m. For the above two cases, no new edge between the two nodes will be established with noncooperative IS, and thus Property 2 follows. ■

B. Application of IS in WLAN-Based IoT

We now detail the implementation of IS at STA, AP, and the central controller, respectively. Note that the interferer is not required to do anything for IS except for CSI and data sharing with the interfered transmitter.

A STA needs to perform six tasks for IS as follows. First, it must construct a list of available networks in terms of the received beacon signals. Second, it must determine whether it is an edge STA or a central STA according to the number of available networks on the list. Third, it should estimate CSI based on the NDP frames sent from nearby APs and feed back this information to the associated AP. Fourth, it should contend for a channel according to the LBT rule. Fifth, it should detect collision/interference from adjacent APs during data transmission. Sixth, it should ask the associated AP for assistance when collision/interference occurs.

It should be noted that only edge STA requests for IM assistance, i.e., the proposed mechanism focuses on the management of interference in the overlapping areas. Compared to the existing IEEE 802.11 protocols, one can see that IS requires only minor modifications of STA, i.e., an increased CSI estimation workload and feedback overhead with respect to the edge STA.

APs are connected to a central controller, and only need to inquire of the controller upon reception of an IM request from their clients. The controller calculates IS. In future WLAN, more processing is expected to move from APs to the controller, i.e., an AP may only be responsible for generating RF signals by following the instructions sent from the controller.

As for the WLAN controller, it maintains $\mathbf{C}$ and $\mathbf{T}$ based on the information received from APs. Upon receiving an IM request from APs, the controller calculates an IS solution following the procedure in Fig. 11. Then, it sends instructions to each interfered AP, based on which proper steering signals are generated.

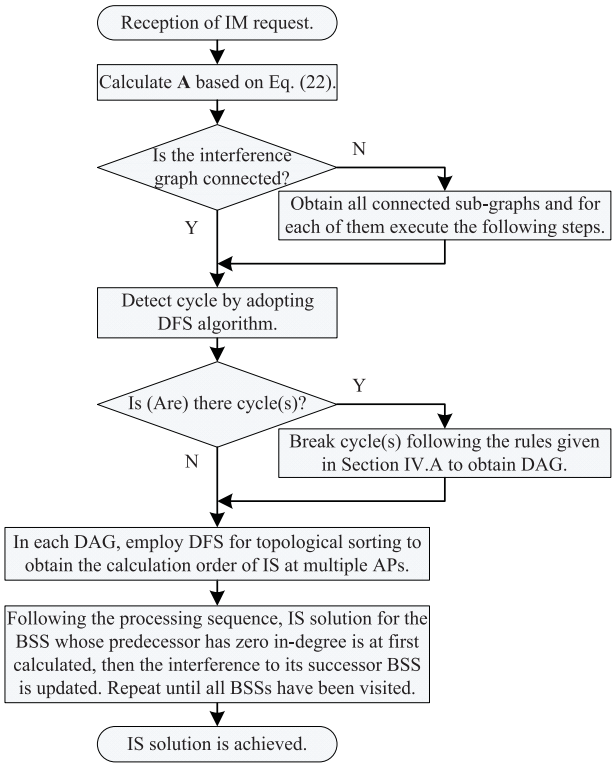

Fig. 11. Flowchart of IS implementation at the WLAN controller.

According to the above discussion, IS can be implemented in WLAN with random network topologies and arbitrary number of interferences. Compared to existing WLAN protocols, the interferer is not required to do anything for IS and only minor modifications are required at the interfered AP and STA. To reduce the scale of interference map and the corresponding processing complexity, we can divide the entire WLAN into multiple subnetworks each of which consists of a limited number of APs. IS is then realized in each part. However, in such a case, interference between subnetworks cannot be managed.

V. Numerical Studies

We evaluate the performance of IS using MATLAB simulation. We set $N_t = N_r = 2$. The system includes K APs with random overlapping areas. All APs have the same transmit power P_T. We define the probability that the element in $\mathbf{A}$ is 1 as p_b. By choosing different p_bs, an interference graph with various interference densities can be generated. Since we focus on IS based on interfered transmitter and the advantages of IS over other noninterfered-transmitter-based implementations have been shown in Section III, here we only study the spectral efficiency of IS and IN in a generalized WLAN with random number and distribution of interferences. It should be noted that with IS or IN, a power overhead will be incurred at the executing AP; when this power cost exceeds P_T, neither IS nor IN is applicable, thus yielding SE $= 0$. In the following discussion, we study the average SE which is computed by using Monte Carlo method, i.e., computing SE $\mathcal{N}$ times for $\mathcal{N}$ channel realizations, and then calculating the average of $\mathcal{N}$ values of SE.

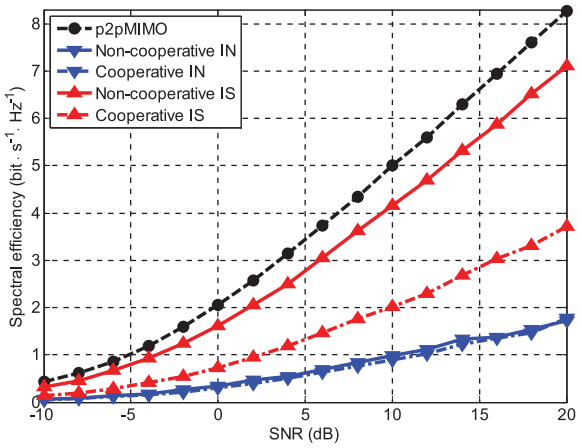

Fig. 12. Single transmission's SE with noncooperative and cooperative IS/IN and single interference.

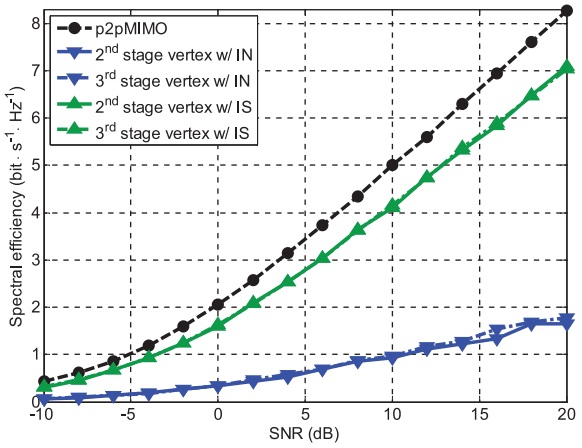

Fig. 13. Single transmission's SE at different processing stages.

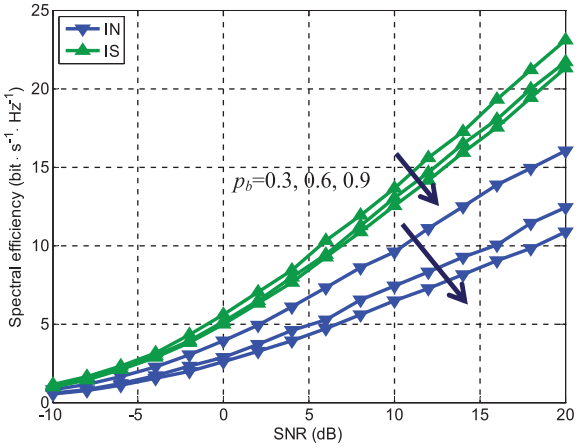

Fig. 14. System SE under $K = 3$, $p_b \in \{0.3, 0.6, 0.9\}$, and $\eta = 2$.

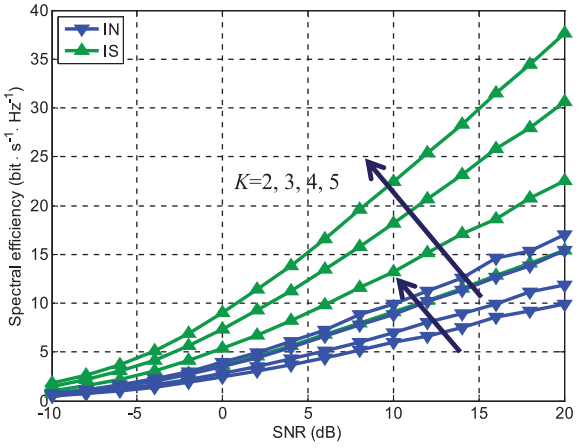

Fig. 15. System SE under $p_b = 0.9$, $K \in \{2, 3, 4, 5\}$, and $\eta = 1$.

Fig. 12 plots the SE of an interfered transmission in a BSS, denoted by a vertex in an interference graph, with noncooperative and cooperative IS/IN and single interference. IS is shown to outperform IN due to the reduced power overhead. Cooperative IS is obviously inferior to noncooperative IS, whereas cooperative and noncooperative IN yield statistically the same SE. This is consistent with the results given in Fig. 8.

Fig. 13 shows the influence of processing stage on an interfered user's average SE. We adopt $K = 3$ and the interference graph with a linear topology. For example, AP_1 disturbs STA_2 associated with AP_2, AP_0 interferes with STA_1 being served by AP_1, and STA_0 associated with AP_0 is free of interference. According to the IS implementation in Fig. 11, since the indegree of v_0 is 0, i.e., interference-free, the IS solution for its successor vertex v_1 should be calculated first, and then v_2. We call v_1 and v_2 the second and third stage vertex, respectively. It can be seen from Fig. 13 that the processing stage does not affect the interfered transmission's SE under either IS or IN. This is because the interfered transmission's SE is dependent on the strength of interference which can be referred to the result given in Fig. 7 where MP_T is the total transmit power of M interferers, but in the given linear topology, the strength of interference incurred to v_1 and v_2 is statically identical.

Fig. 14 plots the average system SE with IS and IN under $K = 3$ and various p_bs. Each interfered receiver suffers from at most two interferences, i.e., $\eta = 2$. SE performance is shown to decrease as p_b increases. Given the same p_b, IS outperforms IN. Moreover, since IS focuses on the mitigation of effective part of interference imposed on the interfered transmission, its SE is not as sensitive to p_b as IN's.

Fig. 15 shows the average system SE with IS and IN under fixed p_b, various K and $\eta = 1$. Although given a fixed p_b, a larger K yields higher CCI among BSSs, since IS can effectively mitigate the influence of interference on each transmission, system SE grows as K increases. Moreover, recall that IS requires much less power than IN, more transmit power will be available for data transmission, and hence IS outperforms IN in SE.

Fig. 16 plots the average system SE with IS and IN under $K = 5$, $p_b = 0.9$, and various η. SE is shown to decrease with increasing η, because as η grows, the aggregated interference is strengthened and more power will be consumed for generating a steering signal. Thus, each interfered transmission's SE decreases, degrading system SE.

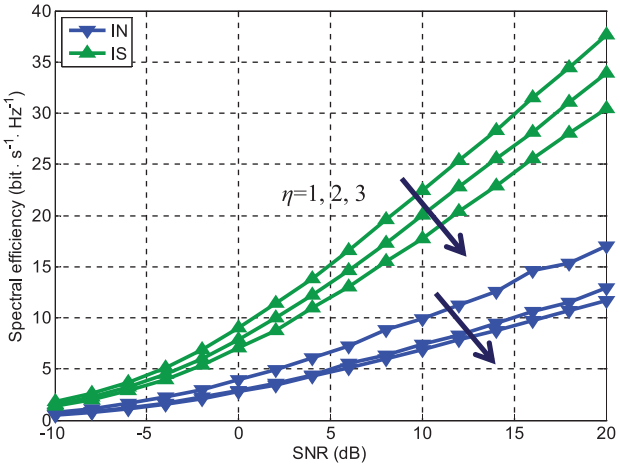

Fig. 16. System SE under $K = 5$, $p_b = 0.9$, and $\eta \in \{1, 2, 3\}$.

VI. Conclusion

In this article, we have proposed and evaluated a novel IM technique, called IS, in IoT. By exploiting both CSI with respect to and data carried in the interference(s), a steering signal is generated so that the spatial feature of interference is made orthogonal to the intended transmission at the interfered receiver. IS does not require any adjustment at the interferer and only minor modifications are required at the interfered transmission pair, thus facilitating its practical implementation and deployment. The proposed mechanism can be applied to general IoT scenarios, e.g., enterprise WLAN, with random network topologies and arbitrary number and distribution of interferences. Our simulation results show that IS can significantly improve system SE over the other existing IM methods.

In this article, we considered the design of IS in the network topology without cyclic, i.e., asymmetric interference situation is assumed, however, in practical use, symmetrical interference topology (also known as X-interference channel) may occur and in such a case how to suppress the negative effect (referred to as a side-effect in this article) of the steering signal to nearby data transmission or even make use of such side-effect to improve the data transmission, is worthy of further study. Moreover, when there are multiple interferences and the interfered receiver can provide multiple DoFs for IM, how to properly allocate DoFs to the steered interferences and desired signals so as to further improve the system's performance needs to be further investigated. These are matters of our future inquiry.

References

[1] "DOCOMO 5G white paper, 5G radio access: Requirements, concept and technologies," NTT DOCOMO, Inc., Tokyo, Japan, 2014.

[2] *5G White Paper*. Accessed: Jun. 2016. [Online]. Available: http://euchina-ict.eu/wp-content/uploads/2015/01/5G-SIG-white-paper-first-version.pdf

[3] S. Liu, L. Xiao, Z. Han, and Y. Tang, "Eliminating NB-IoT interference to LTE system: A sparse machine learning based approach," *IEEE Internet Things J.*, vol. 6, no. 4, pp. 6919–6932, Aug. 2019.

[4] L. Xiao, Y. Li, C. Dai, H. Dai, and H. V. Poor, "Reinforcement learning based NOMA power allocation in the presence of smart jamming," *IEEE Trans. Veh. Technol.*, vol. 67, no. 4, pp. 3377–3389, Apr. 2018.

[5] J. A. Stankovic, "Research directions for the Internet of Things," *IEEE Internet Things J.*, vol. 1, no. 1, pp. 3–9, Feb. 2014.

[6] H. Wang and A. O. Fapojuwo, "Design and performance evaluation of successive interference cancellation-based pure ALOHA for Internet-of-Things networks," *IEEE Internet Things J.*, vol. 6, no. 4, pp. 6578–6592, Aug. 2019.

[7] W. Na, S. Jang, Y. Lee, L. Park, N.-N. Dao, and S. Cho, "Frequency resource allocation and interference management in mobile edge computing for an Internet of Things system," *IEEE Internet Things J.*, vol. 6, no. 3, pp. 4910–4920, Jun. 2019.

[8] Y. Liu, X. Kuai, X. Yuan, Y.-C. Liang, and L. Zhou, "Learning-based iterative interference cancellation for cognitive Internet of Things," *IEEE Internet Things J.*, vol. 6, no. 4, pp. 7213–7224, Aug. 2019.

[9] M. Qian, W. Hardjawana, Y. Li, B. Vucetic, J. Shi, and X. Yang, "Inter-cell interference coordination through adaptive soft frequency reuse in LTE networks," in *Proc. IEEE Wireless Commun. Netw. Conf. (WCNC)*, 2012, pp. 1618–1623.

[10] M. I. Kamel and K. M. F. Elsayed, "Performance evaluation of a coordinated time-domain eICIC framework based on ABSF in heterogeneous LTE-advanced networks," in *Proc. Glob. Commun. Conf. (GLOBECOM)*, 2012, pp. 5326–5331.

[11] T. Yoo and A. Goldsmith, "On the optimality of multianntenna broadcast scheduling using zero-forcing beamforming," *IEEE J. Sel. Areas Commun.*, vol. 24, no. 3, pp. 528–541, Mar. 2006.

[12] D. Tse and P. Viswanath, *Fundamentals of Wireless Communication*. Cambridge, U.K.: Cambridge Univ. Press, 2004.

[13] "Further advancements for E-UTRA physical layer aspects; coordinated multiple point transmission and reception," 3GPP, Sophia Antipolis, France, Rep. TR36.814, 2010.

[14] M. Mollanoori and M. Ghaderi, "Uplink scheduling in wireless networks with successive interference cancellation," *IEEE Trans. Mobile Comput.*, vol. 13, no. 5, pp. 1132–1144, May 2014.

[15] G. Bresler, D. Cartwright, and D. Tse, "Feasibility of interference alignment for the MIMO interference channel," *IEEE Trans. Inf. Theory*, vol. 60, no. 9, pp. 5573–5586, Sep. 2014.

[16] V. Ntranos, M. A. Maddah-Ali, and G. Caire, "Cellular interference alignment," *IEEE Trans. Inf. Theory*, vol. 61, no. 3, pp. 1194–1217, Mar. 2015.

[17] C. M. Yetis, T. Gou, S. A. Jafar, and A. H. Kayran, "On feasibility of interference alignment in MIMO interference networks," *IEEE Trans. Signal Process.*, vol. 58, no. 9, pp. 4771–4782, Sep. 2010.

[18] S. Mohajer, S. N. Diggavi, C. Fragouli, and D. N. C. Tse, "Transmission techniques for relay-interference networks," in *Proc. 46th Annu. Allerton Conf. Commun. Control Comput.*, 2008, pp. 467–474.

[19] J. Zhang, Z. K. M. Ho, E. A. Jorswieck, and M. Haardt, "SINR balancing for non-regenerative two-way relay networks with interference neutralization," in *Proc. Int. Conf. Acoust. Speech Signal Process. (ICASSP)*, 2014, pp. 7604–7608.

[20] D. Wu, C. Yang, T. Liu, and Z. Xiong, "Feasibility conditions for interference neutralization in relay-aided interference channel," *IEEE Trans. Signal Process.*, vol. 62, no. 6, pp. 1408–1423, Mar. 2014.

[21] J. Chen, A. K. Singh, P. Elia, and R. Knopp, "Interference neutralization for separated multiuser uplink-downlink with distributed relays," in *Proc. Inf. Theory Appl. Workshop (ITA)*, 2011, pp. 524–532.

[22] T. Gou, S. A. Jafar, C. Wang, S.-W. Jeon, and S.-Y. Chung, "Aligned interference neutralization and the degrees of freedom of the $2 \times 2 \times 2$ interference channel," *IEEE Trans. Inf. Theory*, vol. 58, no. 7, pp. 4381–4395, Jul. 2012.

[23] *Enterprise Mobility 4.1 Design Guide*. Accessed: Sep. 2019. [Online]. Available: https://www.cisco.com/c/en/us/td/docs/solutions/Enterprise/Mobility/emob41dg/emob41dg-wrapper/ch3_WLAN.html#wpxref12674

[24] E. Perahia and R. Stacey, *Next Generation Wireless LANs: 802.11n and 802.11ac*, 2nd ed. New York, NY, USA: Cambridge Univ. Press, 2013.

[25] S. He *et al.*, *CSI Feedback for MIMO-OFDM Transmission in IEEE 802.11aj (45GHz)*, IEEE Standard 802.11-14/1400r1, 2014.

[26] S. Sen, R. R. Choudhury, and S. Nelakuditi, "CSMA/CN: Carrier sense multiple access with collision notification," *IEEE/ACM Trans. Netw.*, vol. 20, no. 2, pp. 544–556, Apr. 2012.

[27] S. Rayanchu, A. Mishra, D. Agrawal, S. Saha, and S. Banerjee, "Diagnosing wireless packet losses in 802.11: Separating collision from weak signal," in *Proc. IEEE Conf. Comput. Commun. (INFOCOM)*, 2008, pp. 1409–1417.

[28] Z. Li, F. Guo, C. Shu, K. G. Shin, and J. Liu, "Dynamic interference steering in heterogeneous cellular networks," *IEEE Access*, vol. 6, pp. 28552–28562, 2018.

[29] Z. Li, X. Dai, and K. G. Shin, "Decoding interfering signals with fewer receiving antennas," in *Proc. IEEE Conf. Comput. Commun. (INFOCOM)*, 2016, pp. 370–378.
[30] Z. Li, Y. Liu, K. G. Shin, J. Li, F. Guo, and J. Liu, "Design and adaptation of multi-interference steering," *IEEE Trans. Wireless Commun.*, vol. 18, no. 7, pp. 3329–3346, Jul. 2019.
[31] J. L. Gross, J. Yellen, and P. Zhang, *Handbook of Graph Theory*, 2nd ed. Boca Raton, FL, USA: CRC Press, 2013.
[32] P. V. Dooren. *Graph Theory and Applications*. Accessed: Sep. 2019. [Online]. Available: www.hamilton.ie/ollie/Downloads/Graph.pdf

Zhao Li (S'08–M'10) received the B.S. degree in telecommunications engineering, and the M.S. and Ph.D. degrees in communication and information systems from Xidian University, Xi'an, China, in 2003, 2006, and 2010, respectively.

He is currently an Associate Professor with the School of Cyber Engineering, Xidian University. He is also with the Shaanxi Key Laboratory of Information Communication Network and Security, Xi'an University of Posts and Telecommunications, Xi'an. He was a Visiting Scholar and then a Research Scientist with the Real-Time Computing Laboratory, Department of Electrical Engineering and Computer Science, University of Michigan, Ann Arbor, MI, USA, from 2013 to 2015. He has published over 40 technical papers at premium international journals and conferences, such as the IEEE TRANSACTIONS ON WIRELESS COMMUNICATIONS, the IEEE INFOCOM, *Computer Communications*, and *Wireless Networks*. His current research interests include wireless communication, 5G communication systems, resource allocation, interference management, Internet of Things, and physical layer security.

Yinghou Liu is currently pursuing the master's degree with the School of Telecommunications Engineering, Xidian University, Xi'an, China.

His current research interests include wireless communication, resource allocation, and interference management.

Kang G. Shin (LF'12) received the B.S. degree in electronics engineering from Seoul National University, Seoul, South Korea, in 1970, and the M.S. and Ph.D. degrees in electrical engineering from Cornell University, Ithaca, NY, USA, in 1976 and 1978, respectively.

He is the Kevin and Nancy O'Connor Professor of Computer Science and the Founding Director of the Real-Time Computing Laboratory, Department of Electrical Engineering and Computer Science, University of Michigan, Ann Arbor, MI, USA, where he has supervised the completion of 82 post-doctorates and also chaired the Computer Science and Engineering Division from 1991 to 1993. From 1978 to 1982, he was on the faculty of Rensselaer Polytechnic Institute, Troy, NY, USA. His current research interests include QoS-sensitive computing and networks, and embedded real-time and cyber-physical systems. He has authored/coauthored over 900 technical articles (over 330 of which are published in archival journals) and over 30 patents or invention disclosures.

Prof. Shin was a recipient of numerous institutional awards and best paper awards. He is a fellow of ACM.

Jia Liu (S'10–M'12) received the Ph.D. degree from the School of Systems Information Science, Future University Hakodate, Hakodate, Japan, in 2016.

He is currently an Assistant Professor with the Center for Cybersecurity Research and Development, National Institute of Informatics, Tokyo, Japan. His current research interests include mobile ad hoc networks, 5G communication systems, D2D communications, Internet of Things, physical layer security, and cyber security. He has published over 20 technical papers at premium international journals and conferences, such as the IEEE TRANSACTIONS ON WIRELESS COMMUNICATIONS, the IEEE TRANSACTIONS ON VEHICULAR TECHNOLOGY, the IEEE INFOCOM, and *Computer Networks*.

Prof. Liu was a recipient of the 2016 IEEE Sapporo Section Encouragement Award and the Best Paper Award of the International Conference on Networking and Network Applications (NaNA) 2017.

Zheng Yan (M'06–SM'14) received the B.Eng. degree in electrical engineering and the M.Eng. degree in computer science and engineering from Xi'an Jiaotong University, Xi'an, China, in 1994 and 1997, respectively, the second M.Eng. degree in information security from the National University of Singapore, Singapore, in 2000, and the Licentiate of Science and the Doctor of Science in Technology degrees in electrical engineering from the Helsinki University of Technology, Helsinki, Finland, in 2005 and 2007, respectively.

She is currently a Professor with Xidian University, Xi'an, and a Visiting Professor with Aalto University, Espoo, Finland. She has authored over 150 peer-reviewed publications and solely authored two books. She is the inventor and co-inventor of over 50 patents and Patent Cooperation Treaty (PCT) patent applications. Her current research interests include trust, security, and privacy, social networking, cloud computing, networking systems, and data mining.

Prof. Yan serves as an Associate Editor of *Information Sciences*, *Information Fusion*, the IEEE INTERNET OF THINGS JOURNAL, IEEE ACCESS, the *Journal of Network and Computer Applications*, and *Security and Communication Networks*. She is a Leading Guest Editor of several reputable journals, including Association for Computing Machinery (ACM) *Transactions on Multimedia Computing, Communications, and Applications*, Future Generation Computer Systems (FGCS), the IEEE SYSTEMS JOURNAL, and Mobile Networks and Applications (MONET). She has served as a Steering, Organization, and Program Committee Member for over 70 international conferences.